The EMBO Journal Vol.16 No.7 pp.1492–1500, 1997

Structure of the complex of an Fab fragment of a neutralizing antibody with foot-and-mouth disease virus: positioning of a highly mobile antigenic loop

Elizabeth A.Hewat[1], Nuria Verdaguer[2], Ignacio Fita[2], Wendy Blakemore[3], Sharon Brookes[3], Andrew King[3], John Newman[3], Esteban Domingo[4], Mauricio G.Mateu[4] and David I.Stuart[5,6]

Institut de Biologie Structurale Jean-Pierre Ebel, 41 avenue des Martyrs, 38027 Grenoble, France, [2]Departamento de Biología Molecular y Celular CID (CSIC), Jordi Girona 18–26, 08034 Barcelona, Spain, [3]Institute for Animal Health, Pirbright Laboratory, Ash Road, Pirbright, Surrey GU24 0NF, UK, [4]Centro de Biología Molecular 'Severo Ochoa' (CSIC-UAM), Universidad Autonoma de Madrid, 28049 Madrid, Spain, [5]Laboratory of Molecular Biophysics, University of Oxford, South Parks Road, Oxford OX1 3QU and [6]Oxford Centre for Molecular Sciences, University of Oxford, South Parks Road, Oxford OX1 3QT, UK

[1]Corresponding author

E.A.Hewat and N.Verdaguer contributed equally to this work

Data from cryo-electron microscopy and X-ray crystallography have been combined to study the interactions of foot-and-mouth disease virus serotype C (FMDV-C) with a strongly neutralizing monoclonal antibody (mAb) SD6. The mAb SD6 binds to the long flexible GH-loop of viral protein 1 (VP1) which also binds to an integrin receptor. The structure of the virus–Fab complex was determined to 30 Å resolution using cryo-electron microscopy and image analysis. The known structure of FMDV-C, and of the SD6 Fab co-crystallized with a synthetic peptide corresponding to the GH-loop of VP1, were fitted to the cryo-electron microscope density map. The SD6 Fab is seen to project almost radially from the viral surface in an orientation which is only compatible with monovalent binding of the mAb. Even taking into account the mAb hinge and elbow flexibility, it is not possible to model bivalent binding without severely distorting the Fabs. The bound GH-loop is essentially in what has previously been termed the 'up' position in the best fit Fab orientation. The SD6 Fab interacts almost exclusively with the GH-loop of VP1, making very few other contacts with the viral capsid. The position and orientation of the SD6 Fab bound to FMDV-C is in accord with previous immunogenic data.

Keywords: antigenicity/cryo-electron microscopy/crystallography/foot-and-mouth disease virus/virus–Fab structure

Introduction

The picornaviruses are small single-stranded RNA viruses of considerable economic and medical importance, some of which exhibit great antigenic variation (Rueckert, 1990). They include poliovirus, rhinovirus, coxsackievirus and hepatitis A virus. Foot-and-mouth disease viruses (FMDVs) constitute the aphthovirus genus of the Picornaviridae and are economically important pathogens of cloven-hoved livestock world-wide (Domingo *et al.*, 1990). With the exception of hepatitis A, the structures of several members of each genus of picornavirus have been determined, including three serotypes of FMDV [isolates O_1BFS (Acharya *et al.*, 1989; Lea *et al.*, 1995), C-S8c1 (Lea *et al.*, 1994) and A22 (Curry *et al.*, 1996)]. The three major capsid proteins of all picornaviruses, VP1, VP2 and VP3, are structurally similar to each other and consist of an eight-stranded β-barrel with a jelly-roll topology (Stuart, 1993). The surface-exposed loops joining the strands of the jelly rolls differ radically between the genera, and to a lesser degree between serotypes. These exposed loops define much of the antigenic character of each virus (for a review, see Mateu, 1995). FMDV differs from the other picornaviruses in having a relatively smooth surface with one exceptionally long exposed loop, the GH-loop of VP1 (residues 134–160), which not only constitutes most of a major antigenic site (Bittle *et al.*, 1982; Pfaff *et al.*, 1982; Stromaier *et al.*, 1982) but also contains a conserved RGD (Arg–Gly–Asp) sequence which has been demonstrated to be essential for attachment of the virus to cells (Mason *et al.*, 1994). This loop is highly disordered in the native virus structure of all serotypes examined to date. When the disulfide bond linking the base of the loop (Cys134) to Cys130 of VP2 is reduced in FMDV-O_1, however, the loop adopts a more highly ordered position lying along the viral surface (Logan *et al.*, 1993). The reduced virus retains most of its infectivity.

For several picornaviruses (some enteroviruses and human rhinoviruses), there is evidence that the receptor-binding site is located at the base of a narrow cleft and it was postulated that these sites are not accessible to antibodies (Rossmann *et al.*, 1985). The major group rhinoviruses [those rhinoviruses which attach to cells via the cell surface receptor molecule intercellular cell adhesion molecule (ICAM-1)], have a continuous depression or canyon around the 5-fold axes and it has been shown that the receptor binds in the canyon (Olson *et al.*, 1993). It has been shown recently (Smith *et al.*, 1996), however, that key viral amino acid residues involved in binding ICAM-1 are also accessible to antibodies; i.e. the receptor site is not effectively hidden from antibodies. Similarly for FMDV, the RGD motif on the GH-loop of VP1 binds both to an integrin receptor and to neutralizing antibodies (Novella *et al.*, 1993). Thus it is apparent that hiding the receptor site is not essential. It is clear, however, that in both the FMDV GH-loop and the rhinovirus 'canyon' there exist adjacent residues which can mutate to give a viable virus particle which escapes detection by particular monoclonal antibodies. Such escape mutations

often occur repeatedly at only a few residue positions (Mateu *et al.*, 1994) and for FMDV-C structural studies have shown that these repeated substitutions tend to occur for residues not involved in interactions with other amino acids (Lea *et al.*, 1994), suggesting that they are not required for maintenance of the capsid structure or for another biological function during the viral life cycle. The concept of a receptor-binding site accessible to antibodies but flanked by residues capable of mutating to give a viable virus which escapes immune surveillance has been proposed previously (Hogle, 1993).

Understanding the mechanisms by which antibodies neutralize picornaviruses and the viruses' escape from antibody recognition requires a detailed knowledge not only of the virus structure but also of the virus–antibody interactions at the amino acid level. The recent studies of viral peptide–antibody complexes (Tormo *et al.*, 1994; Verdaguer *et al.*, 1995; Wein *et al.*, 1995) and picornavirus–antibody complexes (Smith *et al.*, 1996) by X-ray crystallography alone and in combination with cryo-electron microscopy (Smith *et al.*, 1993a,b; Hewat and Blaas, 1996) are contributing to a better understanding of picornavirus neutralization by antibodies. This structural information is complementary to the data obtained by analysis of antibody escape mutants, which have been used to map the viral antigenic sites, and to biochemical studies on the mechanisms of neutralization. Several topologically independent sites have been identified in FMDV-C (see Mateu, 1995). While most amino acid changes which preclude antibody binding occur at the epitope, it has been shown for FMDV-O_1BFS that such substitutions can be located outside the epitope (Parry *et al.*, 1990). A structural explanation for these latter results has been inferred by analysis of escape mutants. It was proposed that the GH-loop exists in different conformations. Mutations outside the GH-loop could switch the population of conformations sampled by this loop from a predominantly 'up' position close to the capsid 5-fold axis (where those mutations were found) to a predominately 'down' position closer to the capsid 2-fold axis (Parry *et al.*, 1990; Logan *et al.*, 1993).

In order to obtain direct information on how monoclonal antibodies (mAbs) interact with FMDV, we have determined the structure of the FMDV-C-S8c1–SD6 Fab complex by combining the results from three-dimensional reconstructions of cryo-electron micrographs and X-ray crystallography. The strongly neutralizing mAb, SD6, was elicited against the virus and binds to a continuous epitope on the GH-loop. The crystal structure of a synthetic peptide representing the GH-loop of FMDV-C complexed with the Fab of mAb SD6 has been determined (Verdaguer *et al.*, 1995). The complexed peptide shows considerable structural similarity to the VP1 GH-loop of the reduced form of FMDV-O and the RGD motif interacts directly with the Fab. In the crystal structure of FMDV-C-S8c1 alone (Lea *et al.* 1994), the GH-loop was disordered and so the structure of the complex described here provides the first information on the structure of this receptor-binding loop in relation to the rest of the virus capsid and further reinforces our picture of the GH-loop of FMDV VP1 acting as a mobile structural module.

Results and discussion

Cryo-electron microscopy of FMDV-C–SD6 Fab complexes

Cryo-electron microscope images of frozen hydrated complexes between FMDV-C and SD6 Fab revealed an extremely homogeneous population of 300 Å diameter spheres uniformly decorated with radially projecting spikes (Figure 1). No empty capsids were observed. The only objects visible in the background were small pentameric clusters of protein (Figure 1). We interpret these as dissociated FMDV pentamers [such 12S particles are produced by acid dissociation of the virus (Vasquez *et al.*, 1979)] complete with five SD6 Fabs attached. Only the Fabs are visible as the FMDV pentamer is too thin to be observed. No partially decomposed FMDV-C–SD6 Fab or RNA were detected. In common with previous evidence that the FMDV capsid does not in general form stable altered capsids (Baxt and Bachrach, 1980), we conclude that FMDV dissociation on binding of SD6 Fab is a rapid, all or nothing, process.

Reconstructed density of the FMDV-C–SD6 Fab complex

Isosurface representations of the FMDV-C–SD6 Fab complex show the nearly spherical FMDV-C decorated with 60 bilobed Fabs which project 80 Å almost radially from the surface (Figure 2). In the reconstruction, the maximum density in the Fab and in the viral capsid are the same, indicating an occupation of the virus with Fab of close to 100%. The isosurface representation of native FMDV-C restricted to 30 Å resolution was calculated from the X-ray structure (Lea *et al.*, 1994) (Figure 3). Compared with related picornaviruses such as human rhinoviruses (Smith *et al.*, 1993a,b; Hewat and Blaas, 1996), FMDV-C has a remarkably smooth surface at low resolution. However, triangular plateaux centred on the 3-fold axes are discernible and there is sufficient surface detail to allow unambiguous determination of the hand of the reconstructed complex.

Location of the Fab on the viral surface

The X-ray structure of the SD6 Fab complexed with the 15mer peptide, which mimics the VP1 GH-loop of FMDV-C-S8c1 (Verdaguer *et al.*, 1995), fits the cryo-electron microscopy density map reasonably well in two orientations related by the pseudo 2-fold axis of the Fab (orientations I and II shown in Figure 4). The correct orientation is not easily distinguished by eye. The missing VP1 GH-loop in the structure of native FMDV-C-S8c1 (see Table 1) (Lea *et al.*, 1994), the quasi-cyclic nature of the peptide in the Fab SD6–peptide complex and the absence of unfavourable interactions for either orientation give no indication of the correct orientation. However, the characteristic elbow angle of the SD6 Fab is discernible in sections of the FMDV–SD6 reconstructed density. The thick section shown in Figure 5 contains the pseudo 2-fold axis of the Fab. The direction of flexion of the Fab elbow is well defined, and a rough estimate of the elbow angle obtained from this section is 163° as determined from the X-ray crystallographic structure (Verdaguer *et al.*, 1996). This implies that the Fab is in orientation I. Also the Fab in orientation I showed a small but consistently better fit

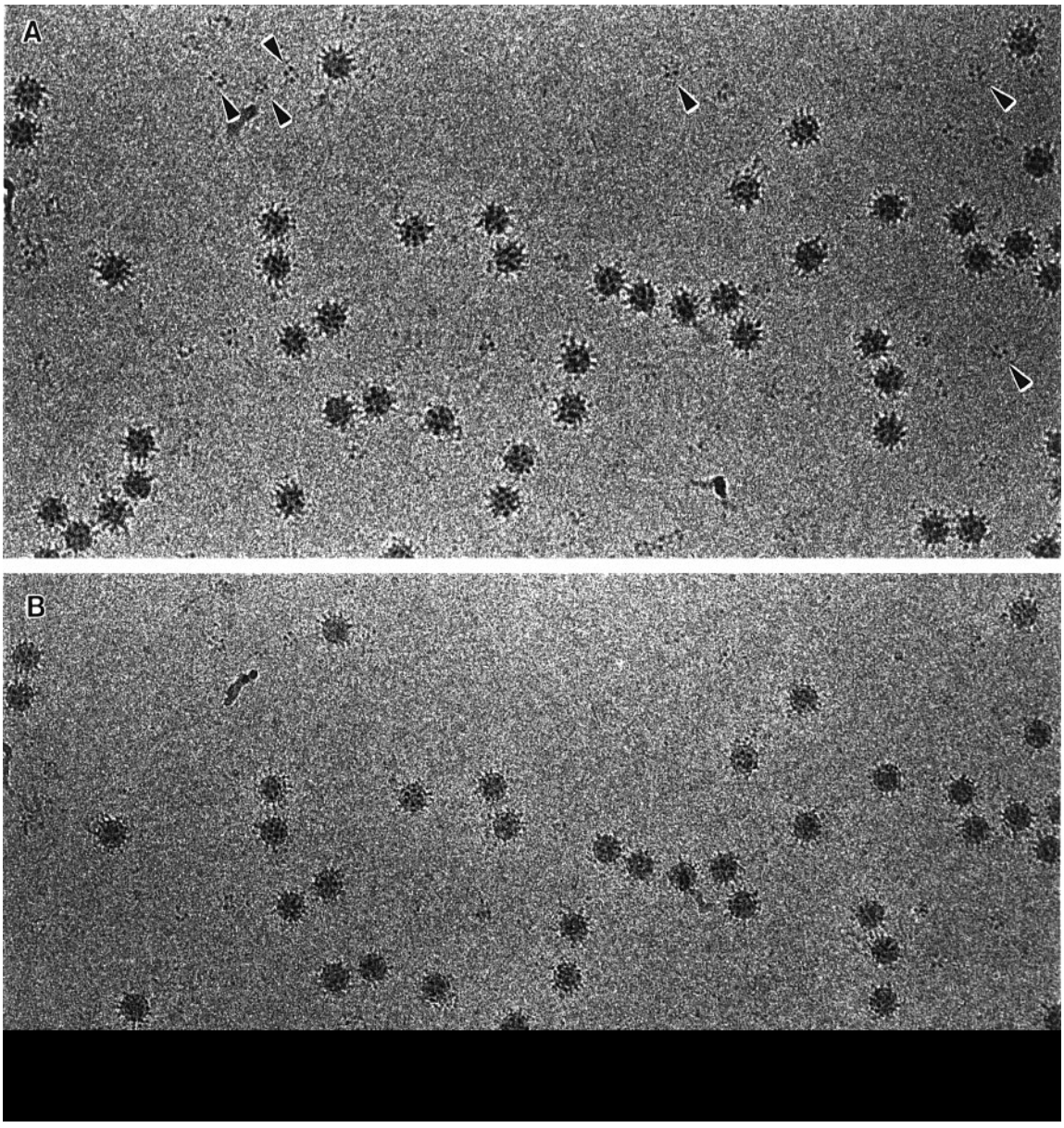

Fig. 1. Electron micrographs of frozen hydrated FMDV-C–SD6 Fab at a defocus of approximately –3.0 μm (**A**) and –1.8 μm (**B**). Note the dissociated pentamers indicated by arrowheads. The scale bar represents 1000 Å.

irrespective of the refinement procedure employed (see Table II and Materials and methods). When the Fab constant and variable modules were allowed to move independently during reciprocal space refinement, orientation I gave a better fit: the elbow angle remained practically unchanged at 163° but, for orientation II, the constant and variable modules were separated by ~4 Å, thus distorting the Fab structure. Orientation I was also strongly supported by the fit of the Fab-bound peptide, whose N-terminus connects directly onto the ordered base of the VP1 GH-loop in the virus at the same location as the corresponding sequence in native FMDV-O_1BFS, where most of the loop is not resolved (Acharya *et al.*, 1989). The fit at the C-terminus of the peptide is also close, requiring only minor reorganization (see Materials and methods). This is permissible, as the ends of the GH-loop not visible in the X-ray structures may be considered as highly flexible. A simple rotation in the plane of the capsid surface would allow the transition between the up and down conformations (Parry *et al.*, 1990; Figure 6). Because all the evidence favours orientation I, the structural analysis that follows is concentrated mainly on this orientation. However, most conclusions are valid for both orientations.

The geometry of SD6 binding precludes bivalent attachment

For orientation I, the shortest distance between the C-terminal ends of the Fab heavy chains is 87 Å for Fab fragments located in the same pentamer, and 91 Å for Fabs related by the icosahedral 2-fold axis. When the Fab elbow angle is changed to the extremely small value of 130°, without moving the Fab variable domains, these distances change to 97 and 61 Å, respectively (Figure 7). All of these distances are too large to allow any two Fab fragments on the same virus particle to be linked together.

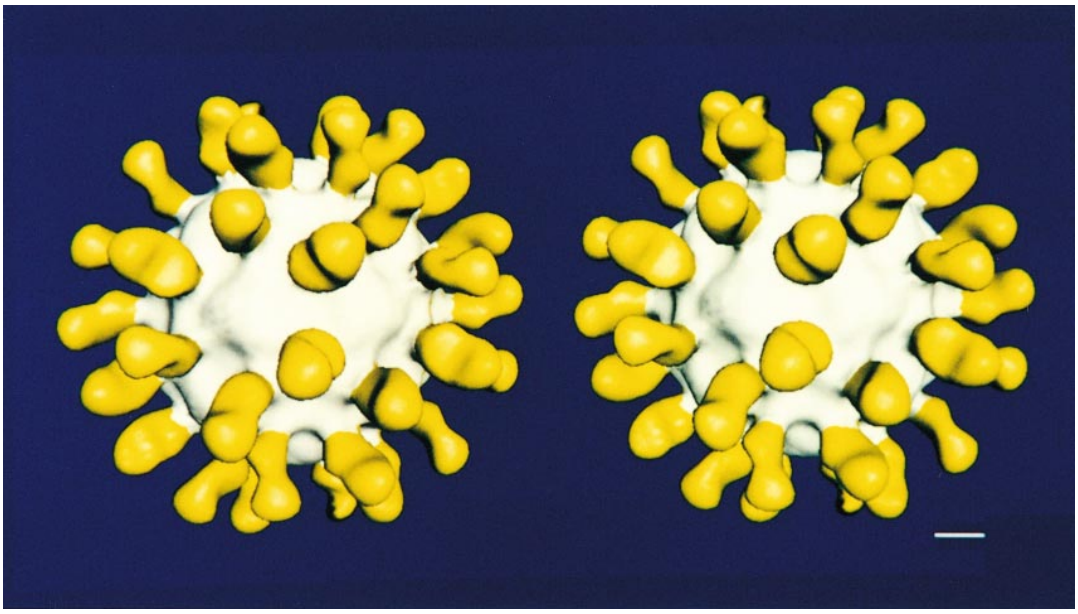

Fig. 2. Stereo view of the isosurface representation of the reconstructed FMDV-C–SD6 Fab complex viewed down a 2-fold axis. The Fab is coloured in yellow ($R > 150$ Å) and the viral capsid ($R < 150$ Å) in white. The scale bar represents 50 Å.

Epitopes on the same pentamer are separated by ~55 Å and epitopes on pentamers related by a viral dyad by some 65 Å. Thus only monovalent binding of mAb SD6 to the viral surface appears feasible. A similar analysis for orientation II leads to the same conclusion.

GH-loop position

The GH-loop in the proposed model differs widely from the disposition of the equivalent loop in reduced FMDV-O (Logan *et al.*, 1993). However, large movement of the loops has already been anticipated in particular for serotype O (Parry *et al.*, 1990). For the Fab in orientation I, the loop is directed towards the viral 5-fold axis and approaches the BC-loop of VP1. The position of the GH-loop in this complex is strikingly similar to that proposed some years ago as the 'up' conformation of the loop in serotype O (Parry *et al.*, 1990), despite the fact that the evidence available then was largely serological; indeed, with the structure of the loop in the reduced type O virus, we now have examples of both the 'up' and 'down' conformations proposed in that paper.

Interactions between the SD6 Fab and FMDV-C

The SD6 Fab footprint on the viral surface has been computed from the molecular area buried during the formation of the complex. Several probe radii, ranging from 1.7 to 3.5 Å, were used to account for the limited resolution of the data available (we estimate that the error in positioning the components of the complex does not exceed 4 Å) (Table III). Apart from residues on the GH-loop, only a few residues, clustered in three regions on the virus, can be involved in interactions with the Fab. The most extensive interactions involve residues from the C-terminus of VP1 from the neighbouring protomer in the same pentamer (Table III). Some residues from the GH-loop of VP3 could also contribute. In addition, the BC-loop of VP1 presents some contact area when using the largest probe radius, but all interatomic distances

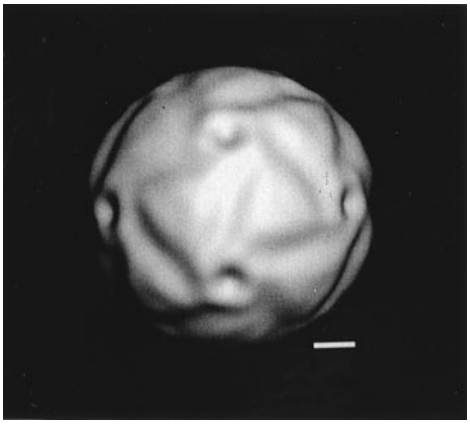

Fig. 3. Isosurface representation of the X-ray map of FMDV-C limited to 30 Å resolution The scale bar represents 50 Å.

between this loop and the Fab are >8.0 Å. For the Fab in orientation II, the pattern of interactions with the viral surface is very similar to that described for orientation I (Table III). The main difference is that in orientation II the interatomic distances between the Fab and the BC-loop are shorter (Table III). It is remarkable that such a small number of interactions suffice to maintain the Fab fragments in a well-determined orientation even during sample preparation for electron microscopy.

The antigenicity of FMDV-C

SD6 binds almost exclusively to a single loop (Table III). This is in contrast to other virus–Fab complexes (Wang *et al.*, 1992; Smith *et al.*, 1993a,b; Wikoff *et al.*, 1994), with the exception of human rhinovirus 2–mAb 8F5 (Tormo *et al.*, 1994; Hewat and Blaas, 1996). The SD6 epitope, in common with several other epitopes of FMDV type C, essentially comprises residues 136–147 of the VP1 GH-loop (Mateu, 1995). The results presented here are in agreement with a variety of previous studies of this

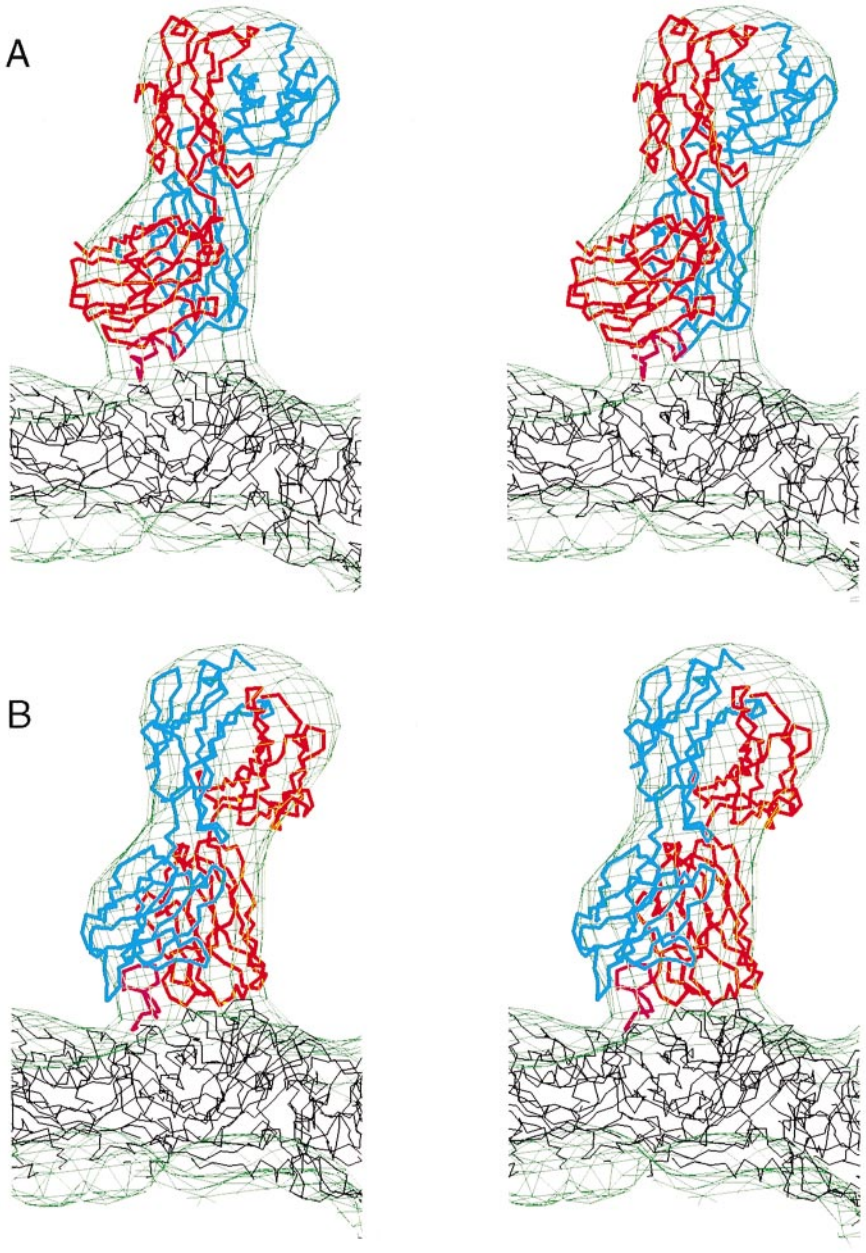

Fig. 4. Stereo views of the complex between FMDV-C-S8c1 and the SD6 Fab with the Fab docked in orientation I (**A**) and II (**B**). The cryo-electron microscope map is represented in green. The C_α tracing of the Fab fragment is indicated in red and blue for the heavy and light chains respectively, and all the viral proteins are shown in black. The synthetic peptide corresponding to the GH-loop of FMDV-C is represented in magenta. The figures were obtained from the program O using O-plot.

epitope. mAbs against this loop in type C virus bind a synthetic peptide and the virion with similar affinity, and all escape substitutions (for a panel of mAbs, including >70 SD6 escape mutants independently derived from C-S8c1) occur within the loop. Antibody competition results revealed little interaction with neighbouring regions of the capsid. The present study, therefore, provides direct structural evidence for what was proposed earlier to be an essentially continuous B cell epitope on a virus capsid (Acharya *et al.*, 1989). Although such structures are not usually found in globular proteins (Barlow *et al.*, 1986), several viruses in addition to FMDV show polypeptide segments, which include immunodominant sites, loosely connected with the rest of the capsid or envelope protein [e.g. canine parvovirus (Strassheim *et al.*, 1994) and

Table I. Structural alignements of the VP1 GH-loops

O reduced	^{130}**YNG**ECRYSRNAVPNLRGDLQVLAQKVARTL**P**^{160}
O oxidized	**YNGEC** RTL**P**^{160}
C virus	**YTG** RHL**P**^{156}
C peptide	^{136}**YTASA** **RGDLAHLTTT**^{150}
CLoop model	**YTGTTAYTASA** **RGDLAHLTTTHARHLP**^{156}

The C peptide includes all 15 residues in the synthetic peptide co-complexed with the SD6 Fab. The CLoop model shows all the GH-loop residues including the three residues TTA at the N-terminus and the two residues HA at the C-terminus of the C peptide missing from the FMDV-C structure. Residues in bold characters are structurally equivalent to residues in the model of the VP1 GH-loop presented in this work.

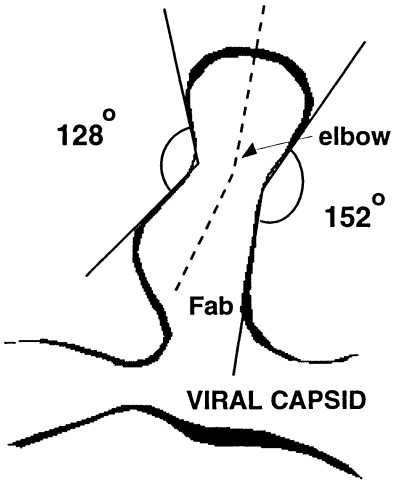

Fig. 5. A thick section of the FMDV–SD6 Fab reconstructed density (isosurface contour) which passes through the pseudo 2-fold axis of the Fab. The apparent elbow angle is indicated with dotted lines.

human immunodeficiency virus (Ghiara *et al.*, 1994)]. The existence of such loops provides encouragement for further attempts at structure-based design of peptide vaccines (Brown, 1992; Mateu, 1995).

The recognition, in isolation, of the GH-loop of FMDV by antibodies does not exclude the possibility that substitutions outside this segment could alter the antigenicity of the loop. This is the case for serotype O, where escape mutations including substitutions towards the C-terminus of VP1 and within or near the BC-loop of VP1, close to the capsid 5-fold axes lead to decreased recognition of the virus by antibodies elicited against the GH-loop presented as a synthetic peptide (Parry *et al.*, 1990; Krebs *et al.*, 1993). Together with structural data, these results were taken to imply that substitutions near the capsid 5-fold axes would destabilize a particular GH-loop structure on the virion, altering the presentation of epitopes within the loop (Parry *et al.*, 1990). It is suggestive that these two VP1 segments include most of the residues closest to the Fab in both orientations derived from the results presented here. Indeed the position of the loop in the favoured orientation resembles the 'up' conformation proposed for native type O virus. Since the type C loop is, however, four amino acids shorter than its counterpart in the O serotype, it remains further from the BC-loop and from all but the last residues of the C-terminal segment of VP1 (Figure 6). It is possible that this is why, in contrast to the observations for the O serotype viruses, no substitutions which impair binding of SD6, or other site A mAbs for type C FMDVs, have been found outside the loop. Such a hypothesis provides a structural explanation for the qualitative differences in antigenicity found between FMDV serotypes.

Antibodies are the host's main defensive weapon against infection by most picornaviruses, including FMDV, and neutralize virus infectivity by a variety of mechanisms. They may, for example, alter virus stability, or interfere with infection by binding to cell attachment sites on the virion, or cross-link virus particles to cause aggregation; yet other antibody-dependent immune mechanisms operate *in vivo* (Dimmock, 1993). In the case of SD6, recent evidence indicates that both the entire antibody molecule and the Fab moiety are strong neutralizers and that they neutralize by interfering with attachment of the virus to cells (N.Verdaguer, unpublished). Thus, while aggregation by SD6 may play a role in neutralization, it is not the only mechanism involved since the Fab fragment is a strong neutralizer. These biochemical observations are fully consistent with the structural data presented here. In particular, both lines of evidence suggest that a bivalent attachment of the antibody to the virus is extremely unlikely and, furthermore, that the paratope of SD6 interacts almost exclusively with the integrin receptor-binding motif.

Table II. Refinement statistics for the complex FMDV-C–SD6 Fab

	Model	1 Body	2 Body
Reciprocal space refinement			
R-factor[a]	I	30.3	29.8
	II	31.3	30.2
R-factor with EM phases[b]	I	33.4	32.1
	II	34.7	33.2
Real space refinement			
R-factor[c]	I	33.9	
	II	34.3	
Correlation coefficient[d]	I	89.2	
	II	88.9	

[a] $R = \Sigma_h||F_{obs}(h)|-k|F_c(h)||/\Sigma_h|F_{obs}(h)|$.
[b] $R = \Sigma_h[A_{obs}(h)-kA_c(h)]^2 + [B_{obs}(h)-kB_c(h)]^2/\Sigma_h|F_{obs}(h)|$.
[c] $R = \Sigma_x|\rho_{obs}(x)-\rho_c(x)|/\Sigma_x\ 2\ |\rho(x)|$.
[d] $CC = \Sigma_x[\rho_{obs}(x) + \rho_c(x)]^2/\Sigma_x\ 2[\rho_{obs}(x)^2 + \rho_c(x)^2]$.

Materials and methods

Preparation of virus and antibody

FMDV-C-S8c1 was purified using the standard procedures described by Curry *et al.* (1992). Neutralizing monoclonal antibody SD6 was elicited against intact FMDV-C-S8c1 virus (Mateu *et al.*, 1987) and its Fab fragment was prepared as described in Verdaguer *et al.* (1994). Note that throughout the text, FMDV-C-S8c1 is often abbreviated to FMDV-C.

Preparation of FMDV-C–SD6 Fab complexes

The FMDV-C–SD6 Fab complex was prepared and purified as described previously (Hewat and Blaas, 1996). FMDV-C (33 μg) and SD6 Fab were incubated at a molar ratio of 1:200 in a volume of 50 μl for 1 h at room temperature. Excess Fab was removed by passage through a Sephacryl S300 spun column (Pharmacia).

Preparation of frozen hydrated specimens

Frozen hydrated specimens were prepared on holey carbon grids as described previously (Hewat *et al.*, 1992a). The holey carbon films, supported on 400 mesh grids, were not glow discharged before use. Samples of the virus suspension (4 μl) were applied to grids, blotted immediately with filter paper for 1–2 s and plunged rapidly into liquid ethane cooled by nitrogen gas at –175°C. Specimens were photographed at a temperature of close to –180°C using a Gatan single-tilt cryo-holder in a Jeol 1200 EX operating at 100 kV. Images were obtained under low dose conditions (<20 e/Å^2) at a nominal magnification of 30 000 times at ~1.8 and 3.0 μm underfocus. All the experimental work involving FMDV-C, including the electron microscopy, was performed under P4 laboratory conditions at The Institute for Animal Health, Pirbright.

Image analysis

Preliminary selection of micrographs, digitization and preparation of virus particle images for analysis was performed as described previously (Hewat *et al.*, 1992b). The pixel size of 20.9 μm on the micrograph corresponds to a nominal pixel size of 6.97 Å/pixel at the specimen. Further image analysis was performed on a DEC Alpha workstation

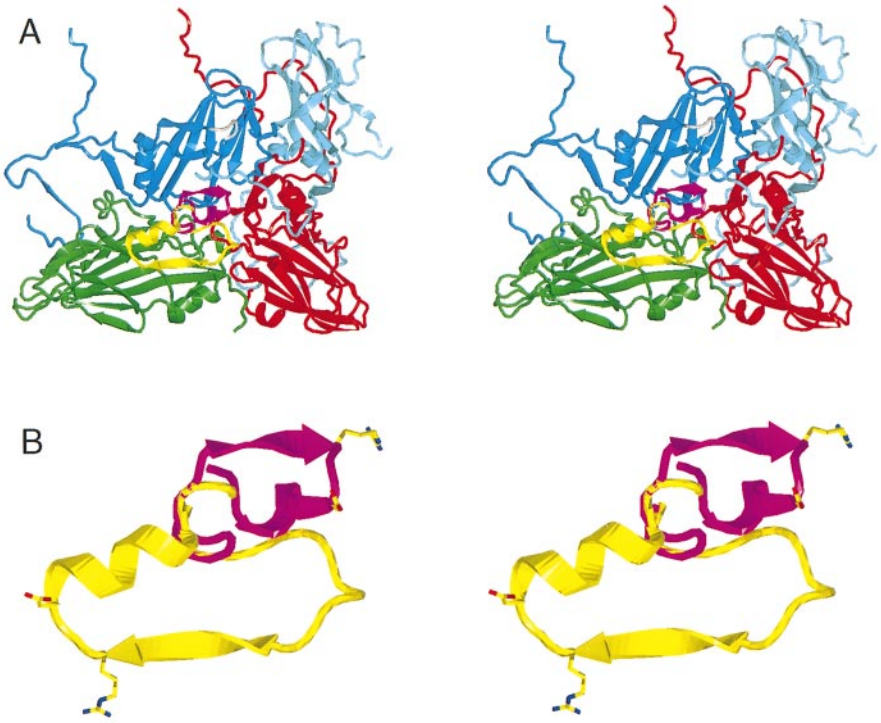

Fig. 6. (**A**) Stereo view of a ribbon protein diagram (obtained with the program O) of the viral proteins VP1 (blue), VP2 (green) and VP3 (red). The VP1 GH peptide derived from the reconstructed model is shown in magenta. For comparison, the conformation of the GH-loop determined in the crystallographic structure of the reduced FMDV-O_1BFS is indicated in yellow. The BC-loop of VP1 is indicated in light grey. The VP1 protein of a neighbouring protomer whose C-terminus interacts with the Fab (see text) is also included (grey). (**B**) Enlarged stereo view of the relative dispositions of the VP1 GH-loops. The orientation and colour codes are as in (A). The side chains of arginine and aspartic from the essential RGD sequence are explicitly shown.

using modified versions of the MRC icosahedral programs and the model-based orientation determination programs (Baker and Cheng, 1996) supplied by S.Fuller (Fuller, 1987; Fuller *et al.*, 1996). For the high defocus image, the orientations and origins of each particle were determined and refined by the method of common lines (Crowther, 1971). The image pair closer to focus was analysed using the orientations determined at the higher defocus as starting data. The lower defocus data was then refined further through several cycles using the model-based orientation determination approach. The best reconstruction used 30 particles and included information to 30 Å resolution. The phase residual went to 90° at this resolution and all the inverse eigenvalues were <0.1. Isosurface representations of the reconstructed density were visualized using Explorer on a Silicon Graphics workstation.

Fitting the FMDV-C and SD6 Fab X-ray structures to the cryo-electron microscopy density

Normalizing the cryo-electron microscopy density map. First, the precise magnification of the electron microscope reconstructed density map of the complex was determined. The reconstructed map was scaled to the X-ray data by comparing the FMDV-C capsid density only. The radially averaged densities within a spherical shell from a radius of 110 to 145 Å were compared by cross-correlation. This gave a pixel size of 6.75 $\pm$0.03 Å/pixel. Secondly, a correction for the effect of the contrast transfer function (CTF) on the cryo-electron microscopy reconstruction was estimated by comparing the reconstructed density map of the complex with the equivalent X-ray map. An X-ray map of the FMDV-C–SD6 Fab complex was created by fitting the X-ray structure of the SD6 Fab into the reconstructed map using the program O on a Silicon Graphics workstation (Jones *et al.*, 1991). The reconstructed map was masked in order to exclude all density except that corresponding to the capsid and the Fab. This was done by subtracting the mean density from the reconstructed map and setting all density below zero to zero. The density <110 Å (corresponding to the viral RNA) was also set to zero. The Fourier transform of identical projections of both maps (i.e. the masked reconstructed map and the equivalent X-ray map) were compared and the ratio of the radially averaged amplitude was smoothed to give a radial CTF correction for the reconstructed map.

Reciprocal space fitting. The structure factors corresponding to the cryo-

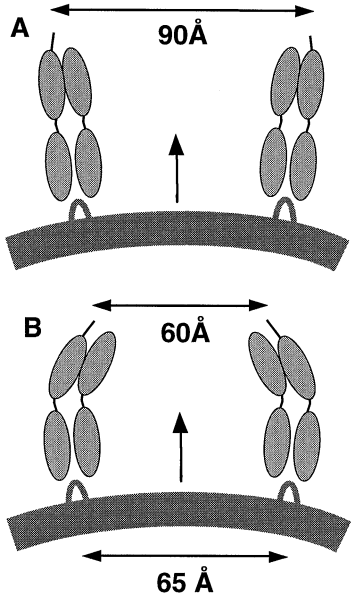

Fig. 7. Schematic drawing indicating the relative positions of two Fab fragments on either side of the icosahedral 2-fold axis. Two light chain domains and two heavy chain domains are represented for each Fab. The constant Fab domains, with a distance of 91 Å between carboxy-terminal residues of the heavy chains, corresponds to orientation I (**A**). When the Fab elbow angle is bent to the extreme value of 130°, the constant modules of neighbouring Fabs approach each other giving a distance of 61 Å (**B**). Thus the Fab fragments cannot be linked together.

Table III. Interactions between SD6 and FMDV-C outside the GH-loop

Virus residues	Buried area probe radius		SD6 contact regions	Cut-off distance (Å)
	1.7 Å	3.5 Å		
Model I				
VP1-Ser45	–	33	CDRL1	8.5
VP1-Asp46	–	18	CDRL1	8.5
VP1-Gln48	–	29	CRDL1	8.5
VP1-Lys206	43	49	CDRL1, CDRL3	3.5
VP1-Gln207	37	45	CDRL1	3.5
VP3-Glu174	6	40	CDRH2	5.0
VP3-Ala175	10	48	CDRH2	5.0
VP3-Thr177	2	28	CDRH2	8.5
Model II				
VP1-Ser45	13	54	CDRH1	5.0
VP1-Asp46	23	56	CDRH1	5.0
VP1-Gln48	32	48	CRDH1	5.0
VP1-Thr50	15	40	CDRH1	5.0
VP1-Ala204	15	52	CDRH2	3.5
VP1-Lys206	71	138	CDRH2	3.5
VP1-Gln207	23	63	CDRH2	3.5
VP3-Glu173	–	21	CDRH3	5.0
VP3-Ala175	–	29	CDRH3	5.0
VP3-Thr177	–	27	CDRH2	8.5

electron microscope density of the virus–Fab complex were calculated by inverse Fourier transformation. These structure factor amplitudes and phases were used to fit the X-ray structures using X-PLOR (Brünger, 1993) rigid-body minimization with the appropriate 60 non-crystallographic symmetry operators. Strict icosahedral symmetry was always imposed and the model of the viral shell was kept fixed. The *R*-factors of the initial and refined models are summarized in Table II. The Fab fragment was treated either as a single rigid body or as two rigid bodies allowing the constant and variable modules to move independently. Refinements were performed both including and excluding the experimental phases (Table II).

Real space fitting. Calculated electron density distributions for both starting models (orientations I and II) were fitted into the cryo-electron microscopy density by a steepest descent procedure which optimized the linear correlation coefficient between the two distributions (Program GAP, J.Grimes and D.I.Stuart, unpublished). A small rotation of ~5° was required to optimize the fitting. Results were closely parallel to those obtained in reciprocal space (Table II). The *R*-factor in real space (Table II) is essentially a measure of the average difference between the ρ_{obs} and ρ_c expressed as a percentage of ρ, and in this case closely parallels the reciprocal space *R*-factor. The cross-correlation coefficient, a commonly used measure of similarity in real space, is essentially an evaluation of 1 minus the square of the difference between ρ_{obs}/ρ and ρ_c/ρ. The cross-correlation coefficient gives a more optimistic evaluation of the similarity, and the real space *R*-factor a more linear evaluation of the percentage difference between ρ_{obs} and ρ_c.

GH-loop modelling

The VP1 GH-loop was assumed to adopt essentially the conformation found for the 15mer peptide complexed with the SD6 Fab. The location of the peptide with respect the viral surface was defined by the rigid-body refinement. Modelling was thus limited to linking both ends of the peptide to the known structure of VP1 (Table I). Three residues (Thr133, Thr134 and Ala135) at the N-terminus of the peptide and two residues (His151 and Ala152) at the C-terminus were missing from the FMDV-C structure. These residues were introduced using complementary information provided by the X-ray structure of oxidized FMDV-O (Table I). The N-terminal region of the peptide could be linked directly to the virus, and regularization done using TURBO (Rousel and Cambillau, 1991) introduced only marginal displacements. In contrast, the connection at the C-terminal end of the peptide required larger rearrangements of residues Arg153, His154 and Leu155.

Acknowledgements

We wish to thank S.Fuller for supplying his latest versions of the MRC icosahedral programs and R.H.Wade for support. This work was funded in part by the DGICYT (grants PB92-0707 and PB94-0034-C02-0), MAFF and Fundación Ramón Areces. N.V. thanks the EMBO for fellowships ASTF8089 and ASTF8375.

References

Acharya,R., Fry,E., Stuart,D., Fox,G., Rowlands,D. and Brown,F. (1989) The three dimensional structure of foot-and-mouth disease virus at 2.8 Å resolution. *Nature*, **337**, 709–716.

Baker,T.S. and Cheng,R.H. (1996) A model based approach for determining orientations of biological macromolecules imaged by cryoelectron microscopy. *J. Struct. Biol.*, **116**, 120–130.

Barlow,D.J., Edwards,M.S. and Thornton,J.M. (1986) Continuous and discontinuous antigenic determinants. *Nature*, **322**, 747–748.

Baxt,B. and Bachrach,H.L. (1980) Early interactions of foot-and-mouth disease virus with cultured cells. *Virology*, **104**, 42–55.

Bittle,J.L., Houghten,R.A., Alexander,H., Shinnick,T.M., Sutcliffer,J.G., Lerner,R.A., Rowlands,D. and Brown,F. (1982) Protection against foot-and-mouth disease virus by immunization with a chemically synthesized peptide predicted from the viral nucleotide sequence. *Nature*, **298**, 30–33.

Brown,F. (1992). New approaches to vaccination against foot-and-mouth disease virus. *Vaccine*, **10**, 1022–1026.

Brünger,A.T. (1993) *XPLOR Manual. Version 3.1*. Yale University, New Haven, CT.

Crowther,R.A. (1971) Procedures for three-dimensional reconstruction of spherical viruses by Fourier synthesis from electron micrographs. *Phil. Trans. R. Soc. Lond. Ser. B*, **261**, 221–230.

Curry,S. *et al.* (1992) Crystallisation and preliminary X-ray analysis of three serotypes of foot-and-mouth disease virus. *J. Mol. Biol.*, **228**, 1263–1268.

Curry,S. *et al.* (1996) Perturbations in the surface structure of A22 Iraq foot-and-mouth disease virus accompanying coupled changes in host cell specificity and immunogenicity. *Structure*, **4**, 135–145.

Dimmock,N.J. (1993) *Neutralization of Animal Viruses*. Springer-Verlag, Berlin.

Domingo,E., Mateu,M.G., Martinez,M.A., Dopazo,J. and Moya,A. (1990) Genetic variability and antigenic diversity of foot-and-mouth disease virus. In Kursta,K.E., Marusyk,R.G., Murphy,F.A. and Van Regenmortel,M.H.V. (eds), *Applied Virology Research.* Plenum Press, New York, Vol. 3, pp. 223–226.

Fuller,S.D. (1987) The T=4 envelope of sinbis virus is organised by complementary interactions with a T=3 icosahedral capsid. *Cell*, **48**, 923–934.

Fuller,S.D., Butcher,S.J., Cheng,R.H. and Baker,T.S. (1996) Three-dimensional reconstruction of icosahedral particles. The uncommon line. *J. Struct. Biol.*, **116**, 48–55.

Ghiara,J.B., Stura,E.A., Stanfield,R.L., Profy,A.T. and Wilson,I.A. (1994) Crystal structure of the principal neutralization site of HIV-1. *Science*, **264**, 82–85.

Hewat,E.A. and Blaas,D. (1996) Structure of a neutralizing antibody bound bivalently to human rhinovirus 2. *EMBO J.*, **15**, 1515–1523.

Hewat,E.A., Booth,T.F., Loudon,P.T. and Roy,P. (1992a) Three dimensional reconstruction of baculovirus expressed bluetongue virus core-like particles by cryo-electron microscopy. *Virology*, **189**, 10–20.

Hewat,E.A., Booth,T.F. and Roy,P. (1992b) Structure of bluetongue virus particles by cryoelectron microscopy. *J. Struct. Biol.*, **109**, 61–69.

Hogle,J.M. (1993) The viral canyon. *Curr. Biol.*, **3**, 278–281.

Jones,T.A., Zou,Y.J., Cowan,S.W. and Kjeldgaard,M. (1991) Improved methods for building protein models in electron density maps and the location of errors in these models. *Acta Crystallogr.*, **A47**, 110–119.

Krebs,O., Ahl.,R., Straube,O.C. and Marquardt,O. (1993) Amino acid changes outside the G-H loop of capsid protein VP1 of type O foot-and-mouth disease virus confer resistance to neutralization by antipeptide G-H serum. *Vaccine*, **11**, 359–362.

Lea,S. *et al.* (1994) The structure and antigenicity of serotype C foot-and-mouth disease virus. *Structure*, **2**, 123–139.

Lea,S. *et al.* (1995) Structural comparison of two strains of foot-and-mouth disease virus subtype O_1 and a laboratory antigenic variant, G67. *Structure*, **3**, 571–580.

Logan,D. *et al.* (1993) Structure of a major immunogenic site on foot-and-mouth disease virus. *Nature*, **362**, 566–568.

Mason,P.W., Rieder,E. and Baxt,B. (1994) RGD sequence of foot-and-mouth disease virus is essential for infecting cells via the natural receptor but can be bypassed by an antibody-dependent enhancement pathway. *Proc. Natl Acad. Sci. USA*, **91**, 1932–1936.

Mateu,M.G. (1995) Antibody recognition of picornaviruses and escape from neutralization: a structural view. *Virus Res.*, **38**, 1–24.

Mateu,M.G., Rocha,E., Vicente,O., Vayreda,F., Navalpotro,C., Pedroso,E., Enjuanes,L., Giralt,E. and Domingo,E. (1987) Reactivity with monoclonal antibodies of viruses from an episode of foot-and-mouth disease. *Virus Res.*, **8**, 261–274.

Mateu,M.G. *et al.* (1994) Antigenic heterogeneity of a foot-and-mouth disease virus serotype in the field is mediated by a very limited sequence variation at several antigenic sites. *J. Virol.*, **68**, 1407–1411.

Novella,I.S., Borrego,B., Mateu,M.G., Domingo,E., Giralt,E. and Andreu,D. (1993) Use of substituted and tandem-repeated peptides to probe the relevance of the highly conserved RGD tripeptide in the immune response against foot-and-mouth disease virus. *FEBS Lett.*, **330**, 253–259.

Olson,N.H., Kolatkar,P.R., Oliveira,M.A., Cheng,R.H., Greve,J.M., McClelland,A., Baker,T.S. and Rossmann,M.G. (1993) Structure of a human rhinovirus complexed with its receptor molecule. *Proc. Natl Acad. Sci. USA*, **90**, 507–511.

Parry,N., Fox,G., Rowlands,D., Brown,F., Fry,E., Acharya,R., Logan,D. and Stuart,D. (1990) Structural and serological evidence for a novel mechanism of antigenic variation in foot-and-mouth disease virus. *Nature*, **347**, 569–572.

Pfaff,E., Mussgay,M., Bohm,H.O., Schultz,G.E. and Shaller,H. (1982) Antibodies against a preselected peptide recognize and neutralize foot-and-mouth disease virus. *EMBO J.*, **1**, 869–874.

Rossman,M.G. *et al.* (1985) Structure of a common cold virus and functional relationship to other picornaviruses. *Nature*, **317**, 145–153.

Rousel,A. and Cambillau,C. (1991) TURBO. In *Silicon Graphics Directory.* Mountain View, CA.

Rueckert,R.R. (1990) Picornaviridae. In Fields,B.N. and Knope,D.M. (eds), *Virology.* Raven Press, New York, pp. 507–548.

Smith,T.J. *et al.* (1993a) Structure of human rhinovirus complexed with Fab fragments from a neutralizing antibody. *J. Virol.*, **67**, 1148–1158.

Smith,T.J., Olson,N.H., Cheng,R.H., Chase,E.S. and Baker,T.S. (1993b) Structure of a human rhinovirus-bivalently bound antibody complex: implications for viral neutralization and antibody flexibility. *Proc. Natl Acad. Sci. USA*, **90**, 7015–7018.

Smith,T.J., Chase,E.S., Schmidt,T.J., Olson,N.H. and Baker,T.S. (1996) Neutralizing antibody to human rhinovirus 14 penetrates the receptor-binding canyon. *Nature*, **383**, 350–354.

Strassheim,M.L., Gruenberg,A., Veijalainen,P., Sgro,J.Y. and Parish,C.R. (1994) Two dominant neutralizing antigenic determinants of canine parvovirus are found on the three-fold spike of the virus capsid. *Virology*, **198**, 175–184.

Stromaier,K., Franze,R. and Ada,K.H. (1982) Location and characterization of the antigenic portion of the FMDV immunizing protein. *J. Gen. Virol.*, **59**, 295–306.

Stuart,D.I. (1993) Viruses. *Curr. Opin. Struct. Biol.*, **3**, 167–174.

Tormo,J., Blaas,D., Parry,N.R., Rowlands,D., Stuart,D. and Fita,I. (1994) Crystal structure of a human rhinovirus neutralizing antibody complexed with a peptide derived from viral capsid protein VP2. *EMBO J.*, **13**, 2247–2256.

Vasquez,D., Denoya,C.D., LaTorre,J.L. and Palma,E.L. (1979) Structure of foot-and-mouth disease virus capsid. *Virology*, **97**, 195–200.

Verdaguer,N., Mateu,M.G., Bravo,J., Tormo,J., Giralt,E., Andreu,D., Domingo,E. and Fita,I. (1994) Crystallization and preliminary X-ray difraction of a monoclonal antibody Fab fragment against foot-and-mouth disease virus and of its complex with the main antigenic site peptide. *Proteins*, **18**, 201–203.

Verdaguer,N., Mateu,M.G., Andreu,D., Giralt,E., Domingo,E. and Fita,I. (1995) Structure of the major antigenic loop of foot-and-mouth disease virus complexed to anti-virus neutralizing antibody. Direct involvement of Arg–Gly–Asp in the interaction. *EMBO J.*, **14**, 1690–1696.

Verdaguer,N., Mateu,M.G., Bravo,J.E., Domingo,E. and Fita,I. (1996) Induced pocket to accommodate the cell atachment Arg–Gly–Asp motif in a neutralizing antibody against foot-and-mouth disease virus. *J. Mol. Biol.*, **256**, 364–376.

Wang,G., Porta,C., Chen,Z., Baker,T.S. and Johnson,J.E. (1992) Identification of a Fab interaction footprint site on an icosahedral virus by cryoelectron microscopy and X-ray diffraction. *Nature*, **355**, 275–278.

Wikoff,W.R., Wang,G., Parrish,C.R., Cheng,R.H., Strassheim,M.L., Baker,T.S. and Rossmann,M. (1994) The structure of a neutralized virus: canine parvovirus complexed with neutralizing antibody fragment. *Structure*, **2**, 595–607.

Wein,M.W., Filman,D.J., Stura,E.A., Guillot,S., Delpeyroux,F., Crainic,R. and Hogle,J.M. (1995) Structure of the complex between the Fab fragment of a neutralizing antibody for poliovirus type 1 and its viral epitope. *Nature Struct. Biol.*, **2**, 232–243.

Received on 23 September, 1996; revised on 10 December, 1996